Carbohydrate Polymers 81 (2010) 291–299

Contents lists available at ScienceDirect

Carbohydrate Polymers

journal homepage: www.elsevier.com/locate/carbpol

In vivo degradation of banana starch: Structural characterization of the degradation process

Fernanda H.G. Peroni-Okita [a], Renata A. Simão [b], Mateus B. Cardoso [c], Claudinéia A. Soares [a], Franco M. Lajolo [a], Beatriz R. Cordenunsi [a,*]

[a] *Laboratório de Química, Bioquímica e Biologia Molecular de Alimentos, Departamento de Alimentos e Nutrição Experimental, FCF, Universidade de São Paulo, Avenida Lineu Prestes 580, Bloco 14, CEP 05508-900, São Paulo, SP, Brazil*

[b] *Programa de Engenharia Metalúrgica e de Materiais, COPPE, Universidade Federal do Rio de Janeiro, CT-F 209, Cidade Universitária, Ilha do Fundão, Caixa Postal 68.505, 21945-970, Rio de Janeiro, RJ, Brazil*

[c] *LNLS, Laboratório Nacional de Luz Síncrotron, Caixa Postal 6192, CEP 13083-970, Campinas, SP, Brazil*

ARTICLE INFO

Article history:
Received 17 December 2009
Received in revised form 4 February 2010
Accepted 11 February 2010
Available online 4 March 2010

Keywords:
Banana starch
Ripening
Starch granule ultrastructure
C-type starch

ABSTRACT

This work reports the first ultrastructural investigation into the degradation process that starch granules isolated from bananas (cv. Nanicão) undergo during ripening. Starch granules from green bananas had a smooth surface, while granules from ripe bananas were more elongated with parallel striations, as revealed by CSLM and SEM. AFM images revealed that the first layer covering the granule surface is composed of a hard material and, as degradation proceeds, hard and soft regions seem to be repeated at regular intervals. WAXD patterns of banana starches were C-type, and the crystalline index was reduced during ripening. The B-/A-type ratio was increased, indicating the preferential degradation of the A-type allomorph. The branch-chain length distribution showed predominantly short chains of amylopectin (*A* and *B1*-chain). The fa/fb ratio was reduced during degradation, while amylose content was increased. The results allowed a detailed understanding of the changes that starch granules undergo during banana ripening.

1. Introduction

Starch is the most important semi-crystalline storage polysaccharide found in plants. Depending on the botanical source, it can be found in a variety of tissues such as leaves (*Arabidopsis*) (Zeeman, Smith, & Smith, 2007), tubers and roots (cassava, sweet potato, yam) (Peroni, Rocha, & Franco, 2006), fruits (banana, mango) (Bernardes-Silva, Nascimento, Lajolo, & Cordenunsi, 2008; Nascimento et al., 2006) and seeds (rice, maize) (Cardoso, Samios, & Silveira, 2006; Steup, 1988), and it is found in a wide range of shapes and sizes. In unripe bananas, the large amount of starch accumulated during the development of the fruit is rapidly degraded during ripening and converted into soluble sugars. Therefore, this banana behavior can be used as a model to study starch-soluble sugar metabolism (Cordenunsi & Lajolo, 1995).

The physiological, biochemical and ultrastructural changes that occur during the ripening process are highly coordinated. It is likely that several enzymes and more than one metabolic pathway are involved in this complex degradation process. Some of these enzymes, such as α and β-amylases (Cordenunsi & Lajolo, 1995; Nascimento et al., 2006; Purgatto, Lajolo, Nascimento, & Cordenunsi, 2001; Vieira-Júnior, Nascimento, & Lajolo, 2006), isoamylases (Bierhals, Lajolo, Cordenunsi, & Nascimento, 2004) and phosphorylases (Mainardi et al., 2006; Mota et al., 2002), have already been detected in banana pulp at different stages of ripening. There are two current models for starch metabolism reported in the literature: one is based on its degradation during cereal seed germination, and the other one on the mobilization of transitory starch stored in leaves during the night (Steup, 1988; Zeeman et al., 2007). In fruit, however, the mechanism that regulates the starch degradation process is not well established.

Starch granules are composed mainly of two types of glucose polymers: amylose and amylopectin. Amylose is an essentially linear molecule, whereas amylopectin is a much larger and branched polymer (Buléon, Colonna, Planchot, & Ball, 1998). These two macromolecules are packed into semi-crystalline granules, with the amylopectin being responsible for the crystallinity of starch (Gallant, Bouchet, & Baldwin, 1997).

The linear portions of amylopectin chains are involved in the formation of the crystalline lamellae, while the branched region of the polymer is responsible for forming the amorphous region (Cameron & Donald, 1992; French, 1973; Manners, 1989). Repetitive units of alternating crystalline and amorphous lamellae form the blocklet structure. The diameter of these blocklets varies between 20 and

* Corresponding author. Tel.: +55 11 30913656; fax: +55 11 38154410.
E-mail address: hojak@usp.br (B.R. Cordenunsi).

0144-8617/$ – see front matter © 2010 Elsevier Ltd. All rights reserved.
doi:10.1016/j.carbpol.2010.02.022

500 nm depending on starch type and their location in the granule. In addition, this structure probably plays an important role in the resistance of starches to enzymatic hydrolysis (Gallant et al., 1997). Blocklets are embedded in an amorphous matrix arranged in concentric rings (called growth rings) that radiate from a central hilum to the granule surface.

The crystalline structure of starch granules has been investigated by means of wide-angle X-ray diffraction (WAXD) studies (Cardoso, Putaux, Samios, & Silveira, 2007; Cheetham & Tao, 1998; Gallant et al., 1982; Glaring, Koch, & Blennow, 2006; Hoover, 2001; Shujun et al., 2007). Depending on the packing of amylopectin double helices, starches can be classified into A and B-type allomorphs (Buléon, Gerard, Riekel, Vuong, & Chanzy, 1998). The A-type pattern is mainly associated with cereals, mango and tapioca starches, while the B-type pattern is usually obtained from tuber starches (such as potato) and high amylose starches. Another C-type pattern is found in some legumes, and WAXD studies suggest that it consists of a mixture of A- and B-type allomorphs within the same granule (Buléon, Colonna, et al., 1998; Buléon, Gerard, et al., 1998; Simão et al., 2008; Thys et al., 2008).

The structure and topography of starch granules have been extensively studied using a variety of microscopic techniques, including optical microscopy (OM), scanning electron microscopy (SEM), transmission electron microscopy (TEM) and atomic force microscopy (AFM) (Chanzy et al., 2006; Gallant et al., 1997; Li, Vasanthan, Hoover, & Rossnagel, 2003; Ridout, Parker, Hedley, Bogracheva, & Morris, 2006). Starch granules viewed under OM have a characteristic layered structure due to the growth rings. SEM has permitted a detailed characterization of starch surface and morphology. When SEM is associated with AFM, the setup makes it possible to ascertain details of the structure of starch with resolution in the nano- to micrometer scale (Glaring et al., 2006; Ridout, Parker, Hedley, Bogracheva, & Morris, 2004; Tang & Copeland, 2007).

Structural characteristics of starch granules such as crystallinity, chain length distribution, and amylose content are primarily responsible for the variable susceptibility of starch granules to enzymatic degradation. In this study, we report the first ultrastructural characterization of the degradation process that starch granules undergo during banana ripening. Total soluble carbohydrates, as well as the amount of starch, were monitored during process of banana ripening. The general shape of the granules and their concentric growth rings were observed by confocal scanning laser microscopy (CSLM). WAXD was used to determine the crystallinity and the ratio of A- to B-type starch allomorphs. Molecular modifications of the granules during banana ripening were monitored via branch-chain length distribution analyses, while the morphological changes of the granules were observed using scanning electron microscopy (SEM) and atomic force microscopy (AFM). A mechanism for starch degradation during ripening is proposed based on the experimental data.

2. Materials and methods

2.1. Materials

Bananas (*Musa acuminata* AAA cv. Nanicão) were obtained from CEAGESP (Companhia de Entrepostos e Armazéns Gerais do Estado de São Paulo, Brazil) immediately post-harvest. The fruit was washed with sodium hypochlorite solution (5%, w/v) and left to ripen under controlled temperature (20 °C) and humidity (85%). Based on ethylene and CO_2 levels (Nascimento et al., 2006), measured daily, the samples were collected, peeled, sliced, frozen in liquid N_2 and stored at −80 °C for subsequent analyses.

2.2. Carbohydrate content

The starch content of pulp tissue was determined enzymatically as described by Cordenunsi and Lajolo (1995). Soluble sugars were extracted three times with 80% ethanol at 80 °C. After centrifugation, supernatants were mixed and ethanol was evaporated under vacuum using a speed-vac system. The soluble sugar content was analyzed by high pressure liquid chromatography with pulse amperometric detection (HPLC-PAD-Dionex, Sunnyvale, CA, USA), using a PA1 column (Dionex, Sunnyvale, CA, USA) in an isocratic run of 18 mM NaOH for 25 min. Total soluble sugar was determined as the sum of the glucose, fructose and sucrose values. The amylose content was determined by using an enzymatic method from Megazyme (kit K-AMYL 04/06, Megazyme International Ireland Ltd., Wicklow, Ireland).

2.3. Starch granule isolation

Starch granules were isolated from the pulp tissue at two different stages of fruit ripening using 20 mM sodium acetate containing 1% ascorbic acid for homogenization instead of distilled water, as suggested by Hallett, Wegrzyn, and MacRae (1995). In the first stage, starch was extracted from green bananas immediately after harvest. In the second stage, granules were obtained from banana fruit when they had fully ripened 18 days after harvest.

2.4. Analysis of starch size distribution

The starch size distribution was determined using Mie scattering analysis using a Malvern-Mastersizer S long bed Version 2.19 instrument (Malvern Instruments Ltd., Malvern, UK). The starch concentration was approximately 0.2 mg/mL. In order to guarantee their homogeneity, the samples were treated with soft ultrasound radiation during the experiment.

2.5. Wide-angle X-ray diffraction (WAXD)

WAXD diagrams were recorded in a rotating-anode X-ray diffractometer (Rigaku corporation, Danvers, MA, USA) with Ni-filtered Cu Kα radiation (λ = 1.542 Å) operating at 50 kV and 100 mA at the Brazilian Synchrotron Light Laboratory (Campinas, Brazil). Diffraction patterns were recorded during 10 min exposures on a mar345 image plate placed at 200.0 mm away from the sample. Calibration was achieved using an alumina pattern. Measurements were made on samples after water content adjustment by sorption at 90% relative humidity (RH) for ten days in the presence of a saturated sodium chloride solution under partial vacuum. The samples were prepared in thin-walled (0.01 mm) glass capillary tubes (0.7 mm in diameter). The capillary was centrifuged to pack the granules at the bottom and sealed in order to prevent any significant change in water content during the measurement. WAXD profiles were obtained by radial averaging and normalized to the integrated area between $2\theta = 5$ and 40°. The WAXD patterns were used to determine the relative crystallinity and respective amount of A- and B-type allomorphs as described in the literature (Pohu, Planchot, Putaux, Colonna, & Buléon, 2004; Wakelin, Virgin, & Crystal, 1959).

2.6. Amylopectin branch-chain length distribution

Starch was debranched using isoamylase from *Pseudomonas* sp. (Megazyme International Ireland Ltd., Ireland) according to the procedure of Jane et al. (1992). The branch-chain length distribution of amylopectin was calculated following the procedure of Koch, Andersson, and Åman (1998) and Franco, Wong, Yoo, and Jane (2002) and analyzed with a high-performance anion exchange chromatograph equipped with a pulsed amperometric detector

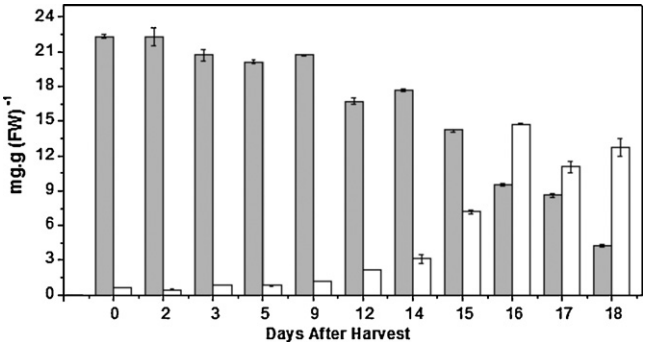

Fig. 1. Relative amounts of starch (gray columns) and soluble sugars (white columns) during ripening of Nanicão bananas. Each column represents the median ($n = 3$) and the bars correspond to the standard error.

(HPAEC-PAD, Dionex, Sunnyvale, CA, USA) according to Jacobs, Eerlinger, Rouseu, Colonna, and Delcour (1998).

2.7. Laser differential interference contrast microscopy

Starch grains suspended in water were placed on a slide and covered by a cover slip. Starch was visualized using a confocal laser scanning microscope (CLSM-LSM 510, Zeiss, Germany) and the images were analyzed with LSMS Image Browser.

2.8. Scanning electron microscopy (SEM)

The samples were fixed in stubs with double-face tape and coated with a 10 nm thick platinum layer with the Bal-tec MED-020 Coating System (Kettleshulme, UK), then analyzed in an FEI Quanta 600 FEG Scanning Electron Microscope (FEI Company, Eindhoven, Netherlands). SEM observations were performed in secondary electron mode operating at 2 kV, 5 kV and 10 kV.

2.9. Atomic force microscopy (AFM)

Starch granules were dispersed in water and fixed on silicon wafers. The surface of the starch granules was observed using a JPK Nano Wizard II, (JPK Instruments AG, Berlin, Germany), equipped with a non-contact AFM probe head and a 100 μm Tripod scanner. The tips (Ultrasharp microprobe) were made of silicon and mounted on a cantilever with a spring constant of 42 N/m and resonance frequencies of 100–160 kHz. Images were processed with Global Lab software (SPO550) (Data Translation Inc., Marlboro, USA).

3. Results and discussion

3.1. Banana starch granules during ripening: quantity, shape and size distribution

The process of starch degradation and its conversion to soluble sugars during ripening of Nanicão bananas are shown in Fig. 1. The amount of starch remains almost constant (around 20%) up to about 14 days, followed by a rapid degradation concomitant with accumulation of soluble sugars. Based on these data, two samples were selected for starch isolation: (1) green bananas (zero days after harvest containing intact starch granules) with ~22% starch and ~0.6% soluble sugars and (2) bananas at the end of ripening process (18 days after harvest containing degraded starch granules) with ~5% starch and ~13% soluble sugars.

Starch granules extracted from green bananas had different morphologies with a predominance of oval and rounded shapes with the growth rings centered on the hilum, as seen in Fig. 2A.

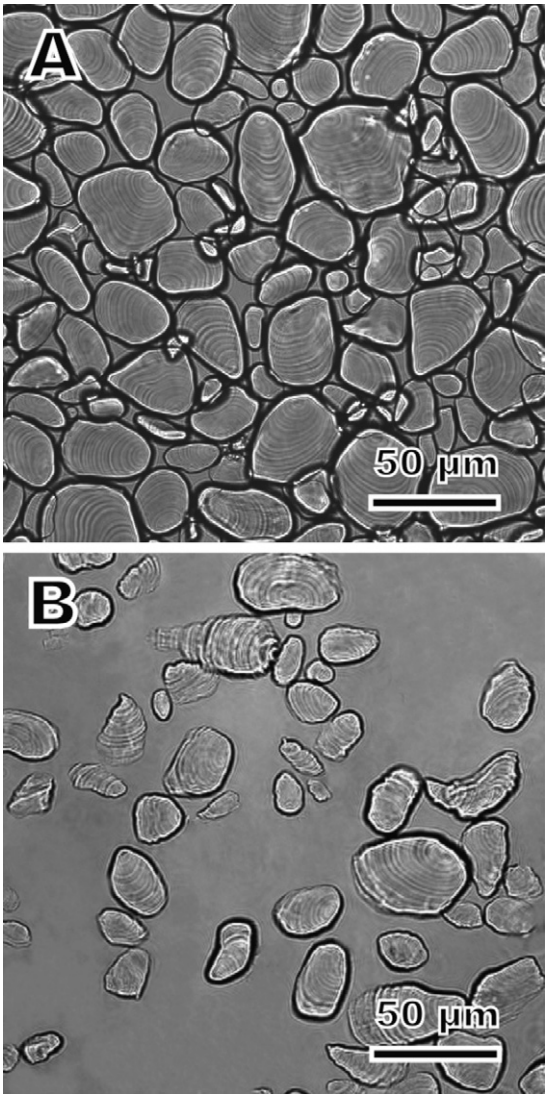

Fig. 2. Laser differential interference contrast micrographs of starch granules isolated from Nanicão bananas obtained (A) immediately after harvest and (B) 18 days after harvest.

Starch granules isolated from bananas in an advanced stage of ripening (18 days after harvest) are presented in Fig. 2B. At this stage, it is observed that some granules are narrowed and elongated, a shape which can be considered characteristic of degraded granules in this cultivar.

Information about the size distribution of the granules was obtained by Mie scattering. By measuring starch granules suspended in water, it was possible to evaluate the granule size distribution (Cardoso et al., 2006; Morelon et al., 2005; Nayouf, Loisel, & Doublier, 2003; Sevenou, Hill, Farhat, & Mitchell, 2002). Table 1 presents the results obtained for starch granules extracted from green and ripe bananas. Starch granules isolated from green bananas displayed an average diameter of approximately 28.9 μm. The granule size distribution indicated that 90% of the granules had diameters smaller than 49.6 μm, whereas 10% of the granules had diameters less than 10.3 μm. The average diameter of the remaining granules from ripe bananas was slightly smaller (25.4 μm) than that from green bananas, as was the size distribution between 10% and 90% of the overall population of granules from ripe bananas (7.6 μm and 45.4 μm, respectively). These results clearly indicate that, even with preferential degradation along the smallest starch axis-dimension (an effect which is not considered in Mie

Table 1
Amylose content, average diameter and size distribution of starch granules isolated from Nanicão bananas at 0 and 18 days after harvest.

Days after harvest	Average diameter (μm)	Size distribution (%)		Crystallinity degree[a] (%)	B/A-type ratio	Amylose content[b] (%)
		90%	10%			
0	28.9	49.6 (μm)	10.3 (μm)	23.6 ± 1.8	1.22	15.1 ± 0.5
18	25.4	45.4 (μm)	7.6 (μm)	21.1 ± 1.9	1.56	15.6 ± 0.3

[a,b] Mean values at least three replicates per sample.

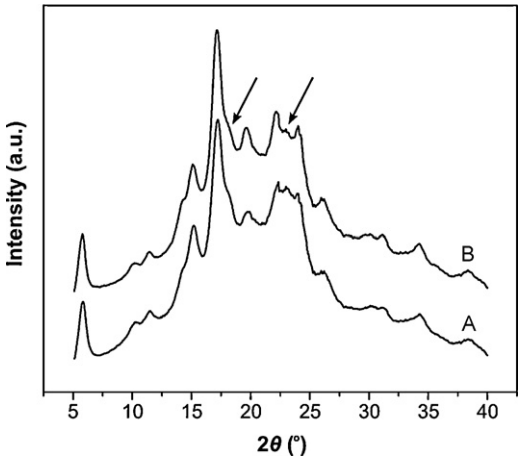

Fig. 3. Wide-angle X-ray diffraction profiles of starch granules extracted from bananas obtained (A) immediately after harvest and (B) 18 days after harvest. The arrows at $2\theta = 18^\circ$ and 23° indicate preferential A-type allomorph degradation during Nanicão banana ripening.

scattering), the longest axial dimension of the granules was also reduced.

3.2. Effects of banana starch degradation on crystallinity, amylose content and branch-chain length distribution of amylopectin

Fig. 3 shows the WAXD patterns of green and ripe banana starch. A typical C-type profile, with peaks characteristic of A- and B-type allomorphs, can be seen for both samples. Table 1 presents the crystallinity index as well as the B-/A-type ratio for each specimen. Green banana starch (Fig. 3A) had a crystalline index of 23.6%, and the proportions of A and B-type allomorphs were 45 and 55%, respectively, with a B-/A-type ratio of 1.22. Fig. 3B shows the WAXD profile of ripe banana starch. Subtle differences could be observed when this was compared to Fig. 3A. Although the C-starch pattern was still recognizable, the intensity of the arrowed A-type peaks at 18° and 23° was slightly reduced. The typical B-type peaks at 5.6, 17.0, 22.0 and 24.0° remained almost constant. The crystallinity index was reduced to 21.1% as a consequence of banana ripening. The A-type content decreased (39%), while the B-type content increased (61%). This led to an increase of the B-/A-type ratio to 1.56. In the literature, it is reported that banana starch can have either an A- or C-type crystallinity pattern depending on the cultivar and the growth conditions, as well as the technique used for granule isolation (Bello-Pérez, Agama-Acevedo, Sáyago-Ayerdi, Moreno-Damian, & Figueroa, 2000; Bello-Perez, Aparicio-Saguilán, Méndez-Montealvo, Solorza-Feria, & Flores-Huicochea, 2005; Jane, Wong, & McPherson, 1997; Millan-Testa, Mendez-Montealvo, Ottenhof, Farhat, & Bello-Pérez, 2005; Zhang, Whistler, BeMiller, & Hamaker, 2005). Bello-Pérez et al. (2000) reported an A-type diffraction pattern for starch isolated from "Macho" and "Criollo" bananas. Later, Bello-Perez et al. (2005) reported a C-type diffraction pattern for "Macho" starch, the same type found by Jane et al. (1997) and Millan-Testa et al. (2005).

The results of branch-chain length distribution of amylopectin in starch isolated from green and ripe bananas are summarized in Table 2. Both samples had 1st and 2nd peak chain lengths of 12–13 and 42–43 DP (degree of polymerization), respectively. According to Hanashiro, Abe, and Hizukuri (1996), branch-chain length distribution can be divided into fractions when analyzed by high-performance anion-exchange chromatography with pulsed amperometric detection: fa, DP 6-12; fb1, DP 13-24; fb2, DP 25-36; fb3, ≥37. These fractions, fa, fb1, fb2 and fb3, correspond to *A*-chains (external short chains), *B1*, *B2* and long *B3*-chains, respectively. Using this classification scheme, the branch-chain length distribution was calculated for starches and is summarized in Table 2.

Amylopectins from green and ripe bananas had a large amount of short *A*- (26% and 25%, respectively) and *B1*-chains (57% and 56%, respectively), and a reduced amount of long *B*-chains (4–5%), as observed by Hanashiro et al. (1996) with starches of different botanical sources. Wang, White, Pollak, and Jane (1993) and Hanashiro et al. (1996) found that the ratios of the fraction, fa/fb1 + fb2 + fb3, can be used to estimate the branch-chain length. Larger ratios indicate an increase in the degree of ramification of amylopectin while a larger proportion of short chains indicate a more crystalline starch granule. In Table 2, the results show that this ratio decreased from 0.35 to 0.33 during starch degradation, which is in agreement with the reduction of the crystallinity index (from 23.6 to 21.1%). This clearly shows that the degree of crystallinity is dependent on the proportion of amylopectin, suggesting that the amount of the fa fraction plays an important role in determining the polymorphic forms of starch crystals. According to Jane et al. (1997) and Sanderson, Daniels, Donald, Blennow, and Engelsen (2006), the branching patterns of amylopectins may play an important role in determining the type of unit packing and the X-ray diffraction pattern, as well as in determining the susceptibility to enzymatic hydrolysis.

Total amylose content (Table 1) remained almost constant in both green (15.1%) and ripe (15.6%) banana starch. These values are in agreement with ones found in other cultivars reported in the

Table 2
Branch-chain length distributions of Nanicão banana starch.

Days after harvest	Peak	DP	Chain length distribution (%)[a]				fa/fb1 + fb2 + fb3[b]
	I[c]	II[c]	dp 6–12	dp 13–24	dp 25–36	dp ≥ 37	
0	12	42	26	57	13	4	0.35
18	13	43	25	56	13	5	0.33

[a] Sum of peak-area ratios (%) of group with degree of polymerization (dp).
[b] Fractionation was as follows: fa, dp 6–12; fb1, dp 13–24; fb2, 25–36; fb3, ≥37.
[c] Maximun degree polimerization at peak.

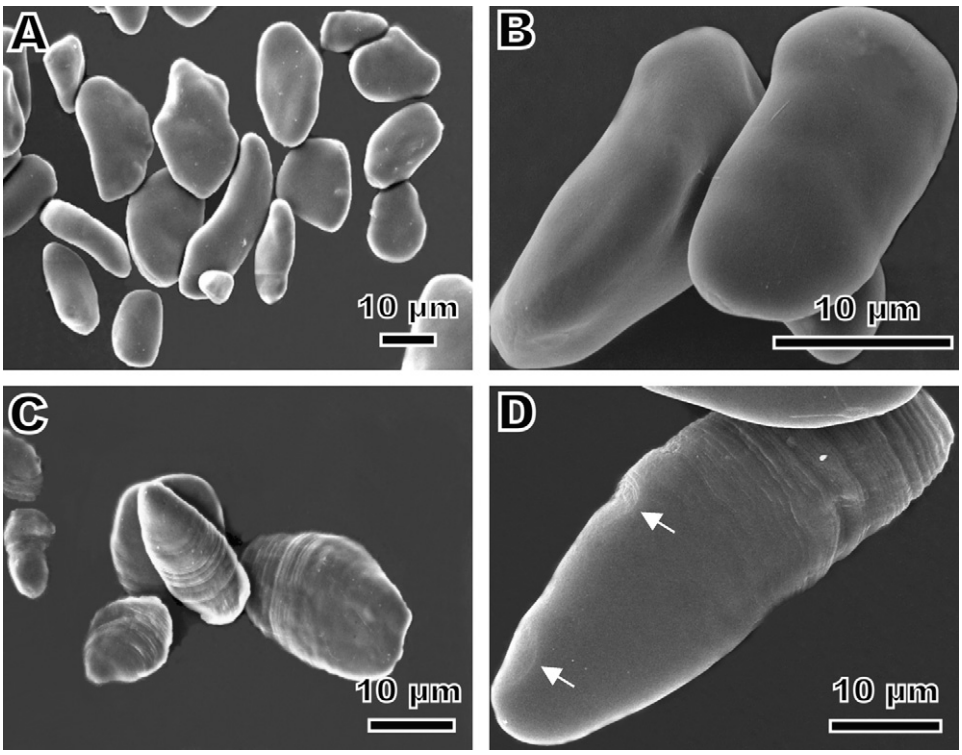

Fig. 4. SEM images of starch granules extracted from Nanicão bananas obtained immediately after harvest (A and B) and 18 days after harvest (C and D). The arrow indicates circular depressions on the granule surface.

literature (Garcia & Lajolo, 1988; Kayisu, Hood, & Van Soest, 1981). However, Waliszewski, Aparicio, Bello, and Monroy (2003) found an amylose content of 40.7% in Valery cv., but those data cannot be compared to the data presented here due to differences in cultivar, stage of fruit ripening and the methodology used to determine the amylose content.

Cheetham and Tao (1998) studied maize starch with different amylose levels and verified the effect of amylose content on the pattern and crystallinity index of starch. The authors showed that when amylose content increased, the scattering intensity of every diffraction peak decreased, except at $2\theta = 20^{\circ}$ which is a diffraction peak that can be related to the formation of amylose–lipid complexes. The results obtained showed no significant reduction in the diffraction peaks of the B-type allomorph and no differences in the amylose content, and we believe that the intensity reduction in the A-type diffraction peaks is related to the preferential degradation of this allomorph.

3.3. Degradation of banana starch granules as viewed by SEM and AFM

Fig. 4A shows SEM images of a population of green banana granules of different shapes (elongated and ovals) and sizes. At higher magnification, Fig. 4B depicts details of the smooth starch granule surfaces. In contrast, starch extracted from ripe bananas showed evidence of degradation through the parallel striations seen in all granules analyzed (Fig. 4C). Fig. 4D shows a typical starch granule in which distinct areas of different degradation patterns were observed. Circular depressions can be seen in the region close to the hilum (indicated by the arrow). On the other side of the granule, the striations are exposed by the degradation process.

Starch striations found on ripe banana starch granules were examined under high magnification showing details of a starch granule in a more advanced process of degradation (Fig. 5). A higher magnification of Fig. 5A is shown in Fig. 5B, in which several layers can be seen on the granule surface. They appear to be in distinct steps of degradation, with progressive layers exposed at regular intervals of about 400 nm. This ordered exposure of layers in the upper portion of the granule suggests that a more resistant region was reached and that the degradation process stopped or became slower at this point. In the opposite region of the granule surface, a smooth and narrowed region is probably a result of the complete degradation of the layers. Fig. 5C shows several granules with distinct pattern of starch degradation. This is probably a result of the initial shape and size of the granules, the degree of granule maturation, the enzymatic degradation and the region of the granule where the enzymes first attacked. Fig. 5D shows another angle of granule degradation, without any measurable distance among layers, most likely because it is located at the end of the top of a rounded granule. This pattern was observed in several images. Fig. 5E and F shows details of a granule in a more advanced stage of degradation than the granule shown in Fig. 5A. The distances between layers increased at regular intervals of 1 μm, however it cannot be explained in light of current knowledge of starch architecture.

Even after a careful analysis of the data, pores were not seen by SEM, showing that the banana starch degradation progresses predominantly layer by layer from the surface to the center of the granule. This clearly indicates that successive layers in the degradation process are organized in an onion-like structure.

Results obtained by AFM (Fig. 6A) shows a topography image of a green banana starch granule with a smooth and low roughness (~30 nm, analyzed by AFM software) surface, reinforced by graphic representation in Fig. 6C (gray line). However, phase contrast microscopy (Fig. 6B) suggests that the granule surface is covered by a likely harder material distributed uniformly on its surface, also shown in Fig. 6C (black line). The whole surface of a ripe banana starch was observed (Fig. 6D) and the demarcated area was analyzed. As ripening progresses, the initial layer is removed by degradation and a new layer can be seen (topography image in

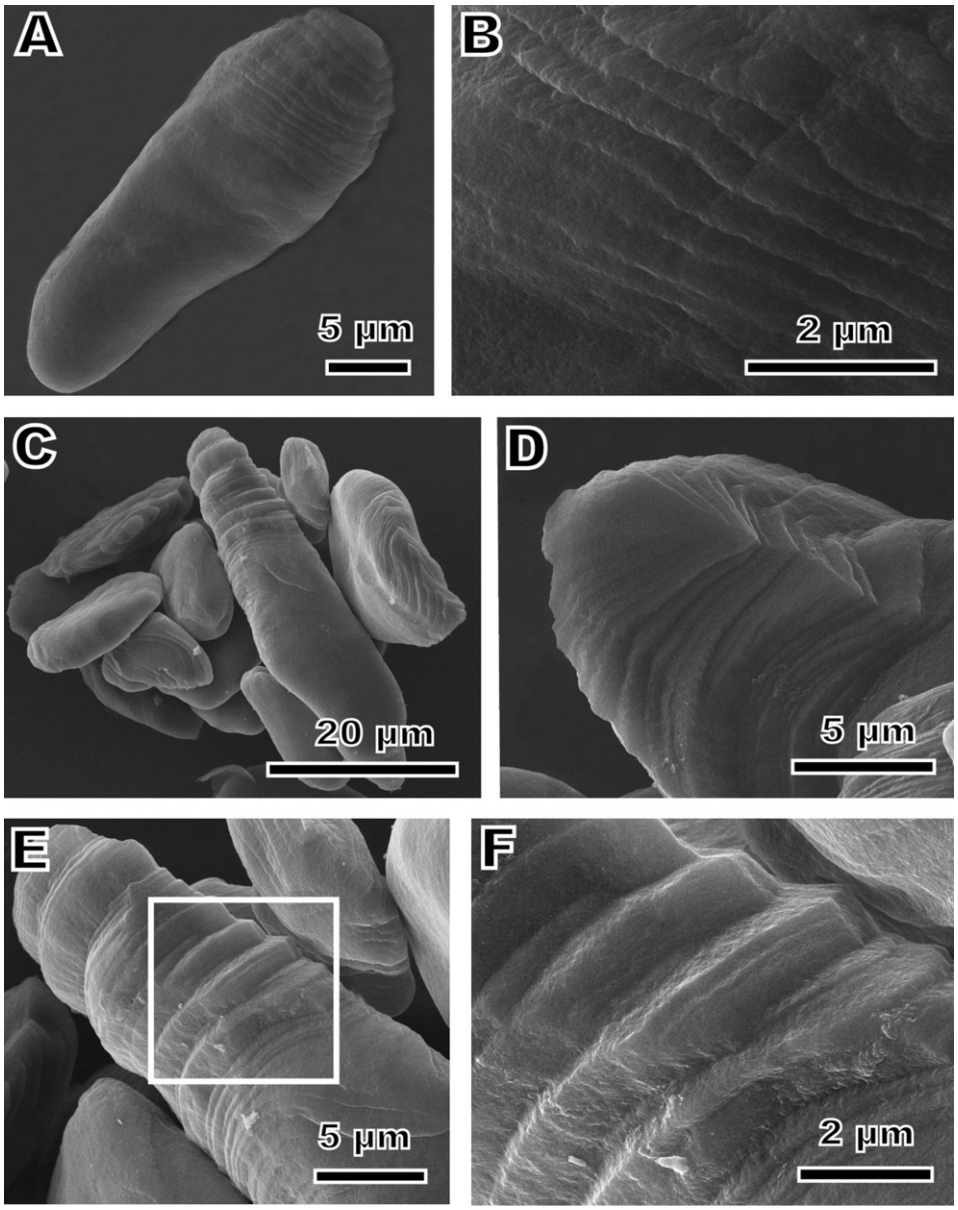

Fig. 5. SEM images of starch granules extracted from Nanicão bananas at 18 days after harvest.

Fig. 6E) revealing repeated regions of approximately 500 nm (Baker, Miles, & Helbert, 2001). The phase contrast image (Fig. 6F) suggests that the new layer exposed through the enzymatic attack is composed by different arrangements of the materials (amylose and amylopectin) producing hard and soft regions, as alternation of bands with different properties inside the layer, like occurs in the growth rings. Because of the phase contrast showing different viscoelastic properties among regions producing repeated regions with the same distance among then (~500 nm), we interpreted that a new layer exposed by the enzymatic degradation is composed by soft and hard regions (black and white arrows, respectively). In the literature we can found starch granules enzymatically hydrolyzed "*in vitro*" by alpha-amylase, producing "ghosts" of the granules with the remained "hard" structure, and the images that we cited is an alternation of growth rings. Here we have the starch granule degradation occurring layer by layer, by a sophisticated enzymatic endogenous apparatus of the banana tissue.

According to Faisant, Gallant, Bouchet, and Champ (1995) and Faisant et al. (1995b), banana starch is known as resistant starch both "*in vitro*" and "*in vivo*" systems (rats and humans). That resistance could be doubt to structural features that difficult the α-amylase activity present in both systems. The authors found that after the passage of banana starch through the small human intestine, the starch granule had their susceptibility to further α-amylase hydrolysis increased. They concluded that the starch granule suffered alterations in their structure that improved the accessibility of some structures. They speculate that this may be due to changes in the granule porosity with no alterations to the integrity of the granules. We think that these changes can be due to changes/degradation of the first layer that covers the granules and turns it more susceptible to the posterior degradation for other enzymes. There is no comparison among the systems that are involved in animal and vegetal complex of starch degradation. Banana starch degradation, for instance is very complex, with several enzymes involved, but studies on starch structure during the degradation "*in situ*" can provide information that will be useful to understand the starch digestion by humans.

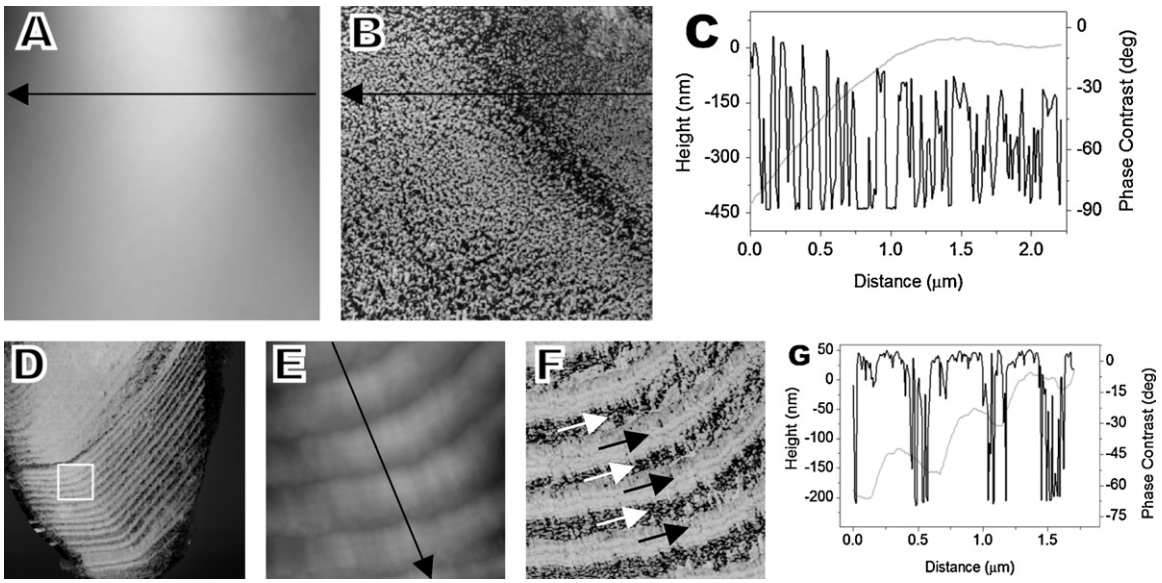

Fig. 6. AFM topography (A) and phase contrast (B) images of starch granule surface immediately after harvest; scan size 2.0 μm × 2.0 μm. (C) Graphic representation of the narrowed area shown in (A and B). (D) AFM phase contrast image of a whole granule surface extracted from Nanicão bananas at 18 days after harvest; scan size 16 μm × 16 μm. AFM topography (E) and phase contrast (F) images showing details of the demarcated area in (D); scan size 2.0 μm × 2.0 μm. (G) Graphic representation of the narrowed area presented in (E and F). The gray and black lines in (C) and (G) represent the topographic and phase contrast images, respectively. The black and white arrows in (F) indicate the soft and hard regions, respectively.

3.4. Starch degradation during ripening: structural evidence for the degradation mechanism

Although the exact mechanism of banana starch degradation is not known due to a large number of variables (temperature, enzymes, amylose content, etc.) that play important roles in this process, the results obtained in this work clearly show the ultrastructural degradation of starch during banana metabolism. As revealed by different microscopic analyses (Figs. 2 and 4), immediately after harvest, the granules from this banana cultivar tend to have predominantly oval and rounded shapes. Once the degradation process starts, starch granules are converted into soluble sugars. In our experiment, this started around the 14th day of ripening (Fig. 1) and eventually became a radial starch degradation (Figs. 2, 4, 5 and 6). A degradation mechanism proposed to explain a partially degraded starch granule with an elongated structure can be explained by the WAXD (Table 1) and AFM (Fig. 6) experiments. At the time that starch granule is degraded, the crystallinity index decreased, and changes in the AFM surface are observed, suggesting that starch degradation occurs preferentially on the granule surface. Although the location of banana starch allomorphs has not been revealed, this scenario is further supported by the distribution of A- and B-type allomorphs in the granule, as observed in C-type pea starch (Bogracheva, Morris, Ring, & Hedley, 1998; Buléon, Colonna, et al., 1998; Buléon, Gerard, et al., 1998). In this way, it can be inferred that A-type crystallites, located on the periphery of starch granules, are preferentially degraded since the granule surface is initially composed of a hard material (Fig. 6B). On the other hand, little degradation of the B-type allomorph, found in the inside of the granule, appears to occur during the ripening process. Thus, a radial degradation of starch can be envisaged that is characterized by preferential reduction of the A-type allomorph (Fig. 3), preferential degradation along the smallest dimensional axis of the granule (Fig. 2) and an increase in soluble sugar in the fruit (Fig. 1). This scenario is also in agreement with the branch-chain length distribution results shown in Table 2, since the short chains of amylopectin (*A* and *B1*-chain) and the fa/fb ratio are reduced concomitantly with a preferential degradation of the A-type allomorph during banana ripening.

In addition, comparison of the green and ripe banana starch granules led us to speculate that the formation of circular depressions and layered striations are related to the availability of soft regions of the granules as viewed by AFM images (Fig. 6F; black arrow). It is likely that when more resistant regions of the granules are reached (Fig. 6F; white arrow), the enzymatic action and degradation process becomes slower or even stops, since the amount of soluble sugars remains almost unchanged and the general starch morphology is not significantly modified at the end of banana ripening. Circular depressions are not observed in green bananas (Fig. 4A and B), and they can be interpreted as defects in the structural arrangement of starch that are susceptible to the initial action of the enzymes involved in starch degradation. We consider that these holes are initiated through α-amylase action and are subsequently enlarged by a complex of others enzymes such as β-amylase and isoamylases, as reported in the literature (Peroni et al., 2008; Zeeman et al., 2007). The layered striations observed at the edges of the granules can be interpreted as a result of this advanced process and as clear evidence of the onion-like structure of starch (Figs. 4–6). Interestingly, the layered striations are commonly observed on the opposite side of the hilum, as depicted in Figs. 4 and 5. This degradation effect is considerably enhanced close to the regions of the granule with a high degree of curvature. We interpret this effect as a discontinuity of the semi-crystalline growth rings that allows easy degradation of the soft imperfect regions of the growth rings. The degradation mechanism presumably occurs until a hard and well-organized semi-crystalline growth ring or a new layer of starch is reached.

4. Conclusions

"*In vivo*" banana starch degradation was studied in order to investigate ultrastructural changes in the granules during fruit ripening. Changes in the proportions of starch and soluble sugars during banana degradation indicates that, from immediately after harvest to the 14th day of ripening, the total amount of starch and soluble sugars are kept almost constant. From the 14th day to the full ripening of the fruits (18 days after harvest), the total availability of sugars increases as a consequence of starch degrada-

tion. Significant differences were observed when starch granules of both green and ripe bananas were compared. Green banana granules tended to have predominantly oval and rounded shapes with a smooth surface, while the ripe bananas had elongated granules with circular depressions and layered striations proposed to be a consequence of their radial degradation. Data from the AFM analysis supported the idea that the first layer covering the granule surface is composed of a hard or well-organized material. Once this first layer is removed by the degradation process, new layers are exposed with hard and soft regions repeated at a regular interval until a hard and well-organized semi-crystalline growth ring or a new layer is reached. As a consequence of the ultrastructural changes of the granules, a subtle decrease of crystallinity and amylopectin branch-chain length were observed during fruit ripening. Although the exact mechanism of banana starch degradation is still unknown, this work represents a significant advance in elucidating the changes in starch granule ultrastructure during "*in vivo*" degradation process.

Acknowledgements

LNLS is acknowledged through the project MX1-6948 (XRD). The authors acknowledge the Fundação de Amparo à Pesquisa do Estado de São Paulo (FAPESP) for financial support and Conselho Nacional de Desenvolvimento Científico e Tecnológico (CNPq) for the scholarship.

References

Baker, A. A., Miles, M. J., & Helbert, W. (2001). Internal structure of the starch granule revealed by AFM. *Carbohydrate Research*, *330*, 249–256.

Bello-Pérez, L. A., Agama-Acevedo, E., Sáyago-Ayerdi, S. G., Moreno-Damian, E., & Figueroa, J. D. C. (2000). Some structural, physicochemical and functional studies of banana starches isolated from two varieties growing in Guerrero, México. *Starch/Stärke*, *52*, 68–73.

Bello-Perez, L. A., Aparicio-Saguilán, A., Méndez-Montealvo, G., Solorza-Feria, J., & Flores-Huicochea, E. (2005). Isolation and partial characterization of mango (*Magnifera indica* L.) starch: Morphological, physicochemical and functional studies. *Plant Foods for Human Nutrition*, *60*, 7–12.

Bernardes-Silva, A. P., Nascimento, J. R. O., Lajolo, F. M., & Cordenunsi, B. R. (2008). Starch mobilization and sucrose accumulation in the pulp of keitt mangoes during postharvest ripening. *Journal of Food Biochemistry*, *32*, 384–395.

Bierhals, J. D., Lajolo, F. M., Cordenunsi, B. R., & Nascimento, J. R. O. (2004). Activity, cloning and expression of an isoamylase-type starch-debranching enzyme from banana fruit. *Journal of Agricultural and Food Chemistry*, *52*, 7412–7418.

Bogracheva, T. Y., Morris, V. J., Ring, S. G., & Hedley, C. L. (1998). The granular structure of C-type pea starch and its role in gelatinization. *Biopolymers*, *45*, 323–332.

Buléon, A., Colonna, P., Planchot, V., & Ball, S. (1998). Starch granules: Structure and biosynthesis. *International Journal of Biological Macromolecules*, *23*, 85–112.

Buléon, A., Gerard, C., Riekel, C., Vuong, R., & Chanzy, H. (1998). Details of the crystalline ultrastructure of C-starch granules revealed by synchrotron microfocus mapping. *Macromolecules*, *31*, 6605–6610.

Cameron, R. E., & Donald, A. M. (1992). A small-angle X-ray scattering study of the annealing and gelatinization of starch. *Polymer*, *33*, 2628–2635.

Cardoso, M. B., Samios, D., & Silveira, N. P. (2006). Study of protein detection and ultrastructure of Brazilian rice starch during alkaline extraction. *Starch/Stärke*, *58*, 345–352.

Cardoso, M. B., Putaux, J. L., Samios, D., & Silveira, N. P. (2007). Influence of alkali concentration on the deproteinization and/or gelatinization of rice starch. *Carbohydrate Polymers*, *70*, 160–165.

Chanzy, H., Putaux, J. L., Dupevre, D., Davies, R., Burghammer, M., Montanari, S., et al. (2006). Morphological and structural aspects of the giant starch granules from *Phajus grandifolius*. *Journal of Structural Biology*, *154*, 100–110.

Cheetham, N. W. H., & Tao, L. (1998). Variation in crystalline type with amylose content in maize starch granules: An X-ray powder diffraction study. *Carbohydrate Polymers*, *36*, 277–284.

Cordenunsi, B. R., & Lajolo, F. M. (1995). Starch breakdown during banana ripening: Sucrose synthase and sucrose phosphate syntase behavior. *Journal of Agricultural and Food Chemistry*, *43*, 347–351.

Faisant, N., Buléon, A., Colonna, P., Molis, C., Lartigue, S., Galmiche, J. P., et al. (1995). Digestion of raw banana starch in the small intestine of healthy humans: Structural features of resistant starch. *British Journal of Nutrition*, *73*, 111–123.

Faisant, N., Gallant, D. J., Bouchet, B., & Champ, M. (1995). Banana starch breakdown in the human small intestine studied by electron microscopy. *European Journal of Clinical Nutrition*, *49*, 98–104.

Franco, C. M. L., Wong, K. S., Yoo, S. H., & Jane, J. L. (2002). Structural and functional characteristics of selected soft wheat starches. *Cereal Chemistry*, *79*, 243–248.

French, D. (1973). Chemical and physical properties of starch. *Journal of Animal Science*, *37*, 1048–1061.

Gallant, D. J., Bewa, H., Buy, Q. H., Bouchet, B., Szlit, O., & Sealy, L. (1982). On ultrastructural and nutritional aspects of some tropical tuber starches. *Starch/Stärke*, *34*, 255–262.

Gallant, D. J., Bouchet, B., & Baldwin, M. (1997). Microscopy of starch: Evidence of a new level of granule organization. *Carbohydrate Polymers*, *32*, 177–191.

Garcia, E., & Lajolo, F. M. (1988). Starch transformation during banana ripening: The amylase and glucosidase behavior. *Journal of Food Science*, *53*, 1181–1186.

Glaring, M. A., Koch, C. B., & Blennow, A. (2006). Genotype-specific spatial distribution of starch molecules in the starch granule: A combined CLSM and SEM approach. *Biomacromolecules*, *7*, 2310–2320.

Hallett, I. C., Wegrzyn, T. F., & MacRae, E. A. (1995). Starch degradation in kiwifruit: In vivo and in vitro ultrastructural studies. *International Journal of Plant Sciences*, *156*, 471–480.

Hanashiro, I., Abe, J. I., & Hizukuri, S. (1996). A periodic distribution of the chain length of amylopectin as revealed by high-performance anion-exchange chromatography. *Carbohydrate Research*, *283*, 151–159.

Hoover, R. (2001). Composition, molecular structure, and physicochemical properties of tuber and root starches: A review. *Carbohydrate Polymers*, *45*, 253–267.

Jacobs, H., Eerlinger, R. C., Rouseu, N., Colonna, P., & Delcour, J. A. (1998). Acid hydrolysis of native and annealed wheat, potato and pea starches—DSC melting features and chain length distributions of lintnerised starches. *Carbohydrate Research*, *308*, 359–371.

Jane, J., Shen, L., Chen, J., Lim, S., Kasemsuwan, T., & Nip, W. K. (1992). Physical and chemical studies of taro starches and flours. *Cereal Chemistry*, *69*, 528–535.

Jane, J. L., Wong, K. S., & McPherson, A. E. (1997). Branch-structure difference in starches of A- and B-type X-ray patterns revealed by their Naegeli dextrins. *Carbohydrate Research*, *300*, 219–227.

Kayisu, K., Hood, L. F., & Van Soest, P. J. (1981). Characterization of starch and fiber of banana fruit. *Journal of Food Science*, *46*, 1885–1890.

Koch, K., Andersson, R., & Åman, P. (1998). Quantitative analysis of amylopectin unit chains by means of high-performance anion-exchange chromatography with pulsed amperometric detection. *Journal of Chromatography A*, *800*, 199–206.

Li, J. H., Vasanthan, T., Hoover, R., & Rossnagel, B. G. (2003). Starch from hull-less barley: Ultrastructure and distribution of granule-bound proteins. *Cereal Chemistry*, *80*, 524–532.

Mainardi, J. A., Purgatto, E., Vieira-Júnior, A., Bastos, W. A., Cordenunsi, B. R., Nascimento, J. R. O., et al. (2006). Effects of ethylene and 1-methylcyclopropene (1-MCP) on gene expression and activity profile of alfa-1,4-glucan-phosphorylase during banana ripening. *Journal of Agricultural and Food Chemistry*, *54*, 7294–7299.

Manners, D. J. (1989). Recent developments in our understanding of amylopectin structure. *Carbohydrate Polymers*, *11*, 87–112.

Millan-Testa, C. E., Mendez-Montealvo, M. G., Ottenhof, M. A., Farhat, I. A., & Bello-Pérez, L. A. (2005). Determination of the molecular and structural characteristics of Okenia, mango, and banana starches. *Journal of Agricultural and Food Chemistry*, *53*, 495–501.

Morelon, X., Battu, S., Salesse, C., Begaud-Grimaud, G., Cledat, D., & Cardot, P. J. P. (2005). Sedimentation field flow fractionation monitoring of rice starch amylolysis. *Journal of Chromatography*, *1093*, 147–155.

Mota, R. V., Cordenunsi, B. R., Nascimento, J. R. O., Purgatto, E., Rosseto, M. R. M., & Lajolo, F. M. (2002). Activity and expression of banana starch phosphorylases during fruit development and ripening. *Planta*, *216*, 325–333.

Nascimento, J. R. O., Vieira-Júnior, A., Bassinello, P. Z., Cordenunsi, B. R., Mainardi, J. A., Purgatto, E., et al. (2006). Beta-amylase expression and starch degradation during banana ripening. *Postharvest Biology and Technology*, *40*, 41–47.

Nayouf, M., Loisel, C., & Doublier, J. L. (2003). Effect of thermomechanical treatment on the rheological properties of crosslinked waxy corn starch. *Journal of Food Engineering*, *59*, 209–219.

Peroni, F. H. G., Koike, C., Louro, R. P., Purgatto, E., Nascimento, J. R. O., Lajolo, F. M., et al. (2008). Mango starch degradation. II. The binding of alpha-amylase and beta-amylase to the starch granule. *Journal of Agricultural and Food Chemistry*, *56*, 7416–7421.

Peroni, F. H. G., Rocha, T. S., & Franco, C. M. L. (2006). Some structural and physicochemical characteristics of tuber and root starches. *Food Science and Technology International*, *12*, 505–513.

Pohu, A., Planchot, V., Putaux, J. L., Colonna, P., & Buléon, A. (2004). Split crystallisation during debranching of maltodextrins at high concentration by isoamylase. *Biomacromolecules*, *5*, 1792–1798.

Purgatto, E., Lajolo, F. M., Nascimento, J. R. O., & Cordenunsi, B. R. (2001). Inhibition of β-amylase activity, starch degradation and sucrose formation by indole-3-acetic acid during banana ripening. *Planta*, *212*, 823–828.

Ridout, M. J., Parker, M. L., Hedley, C. L., Bogracheva, T. Y., & Morris, V. J. (2004). Atomic force microscopy of pea starch: Origins of image contrast. *Biomacromolecules*, *5*, 1519–1527.

Ridout, M. J., Parker, M. L., Hedley, C. L., Bogracheva, T. Y., & Morris, V. J. (2006). Atomic force microscopy of pea starch: Granule architecture of the rug3-a, rug4-b, rug5-a and lam-c mutants. *Carbohydrate Polymers*, *65*, 64–74.

Sanderson, J. S., Daniels, R. D., Donald, A. M., Blennow, A., & Engelsen, S. B. (2006). Exploratory SAXS and HPAEC-PAD studies of starches from diverse plant genotypes. *Carbohydrate Polymers*, *64*, 433–443.

Sevenou, O., Hill, S. E., Farhat, I. A., & Mitchell, J. R. (2002). Organisation of the external region of the starch granule as determined by infrared spectroscopy. *International Journal of Biological Macromolecules*, *31*, 79–85.

Shujun, W., Jinglin, Y., Wenyuan, G., Jiping, P., Hongyan, L., & Jiugao, Y. (2007). Granule structural changes in native Chinese Yam (*Dioscorea opposita* Thunb var, Anguo) starch during acid hydrolysis. *Carbohydrate Polymers*, *69*, 286–292.

Simão, A. S., Bernades-Silva, A. P. F., Peroni, F. H. G., Nascimento, J. R. O., Louro, R. P., Lajolo, F. M., et al. (2008). Mango starch degradation. I. A microscopic view of the granule during ripening. *Journal of Agricultural and Food Chemistry*, *56*, 7410–7415.

Steup, M. (1988). Starch degradation. In *The biochemistry of plants*. San Diego: Academic Press., pp. 255–295.

Tang, M. C., & Copeland, L. (2007). Investigation of starch retrogradation using atomic force microscopy. *Carbohydrate Polymers*, *70*, 1–7.

Thys, R. C. S., Westfahl, H., Jr., Noreña, C. P. Z., Marczak, L. D. F., Silveira, N. P., & Cardoso, M. B. (2008). Effect of the alkaline treatment on the ultrastructure of C-type starch granules. *Biomacromolecules*, *9*, 1894–1901.

Vieira-Júnior, A., Nascimento, J. R. O., & Lajolo, F. M. (2006). Molecular cloning and characterization of an alpha-amylase occuring in the pulp of ripening bananas and its expression in *Pichia pastoris*. *Journal of Agricultural and Food Chemistry*, *54*, 8222–8228.

Wakelin, J. H., Virgin, H. S., & Crystal, E. (1959). Development and comparison of two X-ray methods for determining the crystallinity of cotton cellulose. *Journal Applied Physics*, *30*, 1654–1662.

Waliszewski, K. N., Aparicio, M. A., Bello, L. A., & Monroy, J. A. (2003). Changes of banana starch by chemical and physical modification. *Carbohydrate Polymers*, *52*, 237–242.

Wang, Y. J., White, P., Pollak, L., & Jane, J. (1993). Characterization of starch structures of 17 maize endosperm mutant genotypes with Oh43 inbred line background. *Cereal Chemistry*, *70*, 171–179.

Zeeman, S. C., Smith, S. M., & Smith, A. M. (2007). The diurnal metabolism of leaf starch. *Biochemical Journal*, *401*, 13–28.

Zhang, P., Whistler, R. L., BeMiller, J. N., & Hamaker, B. R. (2005). Banana starch: Production, physicochemical properties, and digestibility—A review. *Carbohydrate Polymers*, *59*, 443–458.